Cancer Therapy: Preclinical

Clinical Cancer Research

SST0001, a Chemically Modified Heparin, Inhibits Myeloma Growth and Angiogenesis via Disruption of the Heparanase/Syndecan-1 Axis

Joseph P. Ritchie[1,2], Vishnu C. Ramani[1], Yongsheng Ren[1], Annamaria Naggi[4], Giangiacomo Torri[4], Benito Casu[4], Sergio Penco[5], Claudio Pisano[5], Paolo Carminati[6], Monica Tortoreto[7], Franco Zunino[7], Israel Vlodavsky[8], Ralph D. Sanderson[1,2,3], and Yang Yang[1,2,3]

Abstract

Purpose: Heparanase promotes myeloma growth, dissemination, and angiogenesis through modulation of the tumor microenvironment, thus highlighting the potential of therapeutically targeting this enzyme. SST0001, a nonanticoagulant heparin with antiheparanase activity, was examined for its inhibition of myeloma tumor growth *in vivo* and for its mechanism of action.

Experimental Design: The ability of SST0001 to inhibit growth of myeloma tumors was assessed using multiple animal models and a diverse panel of human and murine myeloma cell lines. To investigate the mechanism of action of SST0001, pharmacodynamic markers of angiogenesis, heparanase activity, and pathways downstream of heparanase were monitored. The potential use of SST0001 as part of a combination therapy was also evaluated *in vivo*.

Results: SST0001 effectively inhibited myeloma growth *in vivo*, even when confronted with an aggressively growing tumor within human bone. In addition, SST0001 treatment causes changes within tumors consistent with the compound's ability to inhibit heparanase, including downregulation of HGF, VEGF, and MMP-9 expression and suppressed angiogenesis. SST0001 also diminishes heparanase-induced shedding of syndecan-1, a heparan sulfate proteoglycan known to be a potent promoter of myeloma growth. SST0001 inhibited the heparanase-mediated degradation of syndecan-1 heparan sulfate chains, thus confirming the antiheparanase activity of this compound. In combination with dexamethasone, SST0001 blocked tumor growth *in vivo* presumably through dual targeting of the tumor and its microenvironment.

Conclusions: These results provide mechanistic insight into the antitumor action of SST0001 and validate its use as a novel therapeutic tool for treating multiple myeloma. *Clin Cancer Res; 17(6); 1382–93.* ©*2011 AACR.*

Introduction

Multiple myeloma is the second most prevalent hematologic malignancy in the United States (1). The emergence of novel, targeted therapeutics (e.g., bortezomib, thalidomide) has greatly improved survival rates in patients with myeloma (2); however, there is still an unmet need in identifying and developing therapies designed to further prevent the progression of this disease without sacrificing patient quality of life. Recognition that the myeloma tumor microenvironment helps drive the aggressive nature of myeloma has recently led to new strategies for attacking the tumor microenvironment (3). Our lab and others have shown that heparanase, an endo-β-D-glucuronidase that degrades heparan sulfate (HS) chains of proteoglycans (e.g., syndecan-1) on the cell surface and within the extracellular matrix, is rarely expressed in normal tissues, but becomes highly expressed in a number of human malignancies (4), including multiple myeloma (5). Heparanase promotes an aggressive phenotype, in part by synergizing with the heparan sulfate proteoglycan syndecan-1 (CD138) to create a niche within the bone marrow microenvironment further driving myeloma growth and dissemination (6–8). Moreover, work in our lab has shown that active heparanase can be detected in the bone marrow of most myeloma patients and that the presence of high levels of this enzyme correlates with enhanced angiogenic activity, an important promoter of myeloma growth and progression (5). Furthermore, heparanase expression

Authors' Affiliations: [1]Department of Pathology, [2]Center for Metabolic Bone Disease, and [3]Comprehensive Cancer Center, University of Alabama at Birmingham, Birmingham, Alabama; [4]G. Ronzoni Institute for Chemical and Biochemical Research, Milan, Italy; [5]sigma-tau Industrie Farmaceutiche Riunite S.p.A., Pomezia, Italy; [6]sigma-tau Research, Mendrisio, Switzerland; [7]National Cancer Institute, Foundation IRCCS, Milan, Italy; and [8]Cancer and Vascular Biology Research Center, The Bruce Rappaport Faculty of Medicine, Technion, Haifa, Israel

Corresponding Authors: Ralph D. Sanderson, Department of Pathology, University of Alabama at Birmingham, 1530 Third Ave South, SHEL 814, Birmingham, AL 35294. Phone: 205-996-6226; Fax: 205-996-6119; E-mail: sanderson@uab.edu or Yang Yang, Department of Pathology, University of Alabama at Birmingham, 1530 Third Ave South, SHEL 816, Birmingham, AL 35294. E-mail: yangyang@uab.edu

doi: 10.1158/1078-0432.CCR-10-2476

Translational Relevance

This work reports preclinical findings identifying SST0001 as an antiheparanase compound that inhibits myeloma tumor growth *in vivo*. The studies include multiple cell lines and multiple animal models and data that points to mechanisms of action of SST0001. The findings support further investigation of SST0001 in human clinical trials for myeloma and perhaps other cancers where heparanase is upregulated.

within the bone microenvironment is associated with shorter event-free survival of patients with newly diagnosed myeloma treated with high dose chemotherapy and stem cell transplantation (9). Therefore, therapies designed to disrupt the heparanase/syndecan-1 axis in myeloma will likely prove advantageous in the treatment of this devastating disease.

The finding that heparanase is involved in a wide variety of tumor types and is subsequently linked to the development of pathological processes has led to development of therapeutic strategies to inhibit this enzyme (10). Of the compounds produced, only one, PI-88, a phosphomannopentaose sulfate, has entered clinical trials and has not yet been approved for routine clinical use (11–13). Heparin has long been known to possess potent antiheparanase activity (14). Results from several clinical trials using unfractionated heparin and low–molecular weight heparin (LMWH) in preventing pulmonary embolism in advanced stage cancer patients indicated that heparin prolonged survival (15), probably due to a direct effect on the tumor, potentially through inhibition of heparanase enzymatic activity (16). In fact, a recent retrospective study on the effect of anticoagulation on survival in newly diagnosed myeloma patients revealed a possible beneficial effect of LMWH therapy on outcome in myeloma patients (17). Additional preclinical studies have further highlighted the potential use of anticoagulant therapy to treat cancer. Defibrotide, an oligonucleotide anticoagulant, was recently shown to possess *in vivo* chemosensitizing properties and inhibited myeloma growth presumably through inhibiting heparanase activity thereby modulating the tumor microenvironment (18). However, in light of the these findings, use of anticoagulants such as heparin or LMWH as anticancer agents is limited due to the risk of inducing adverse bleeding complications. Fortunately, it is possible to separate the anticoagulant and antiheparanase properties of heparin through a series of chemical modifications (19–21). Nonanticoagulant species of heparin could, therefore, be administered at high doses without risk of causing bleeding disorders. Naggi and coworkers produced a modified heparin that is 100% N-acetylated and 25% glycol split (previously designated ^{100}NA,RO-H, now known as SST0001, sigma-tau Research Switzerland) and is endowed with properties making it suitable for use as a cancer therapeutic. Structural details and heparanase inhibitory activity of this compound have been described (21). Notably, SST0001 potently inhibits heparanase enzymatic activity and exhibits a markedly decreased ability to release and potentiate the mitogenic activity of extracellular matrix-bound FGF-2 as compared with unmodified heparin. Moreover, glycol-splitting causes heparin to lose its affinity for antithrombin with a resulting loss of anticoagulant activity. Collectively, the combination of high inhibition of heparanase, the low release/potentiation of ECM-bound growth factors and the lack of anticoagulant activity points to N-acetylated, glycol-split heparins (e.g. SST0001) as potential antiangiogenic and antimetastatic agents (15). These rationally designed compounds have the potential to be more specific and safer than other heparanase inhibitors.

We now report that SST0001 can effectively inhibit myeloma growth *in vivo*, even when confronted with an aggressively growing tumor within human bone. Importantly, we find that treatment of animals or tumor cells with SST0001 causes changes within tumors consistent with the compound's ability to inhibit heparanase. This included inhibition of expression of HGF, VEGF, and MMP-9 accompanied by diminished angiogenesis and decreased shedding of syndecan-1, a heparan sulfate proteoglycan previously shown to be a potent promoter of myeloma growth (7). Comparison of the molecular size of syndecan-1 from tumor cells treated with or without SST0001 clearly indicates that SST0001 protects the proteoglycan from heparanase-mediated degradation, thus confirming the antiheparanase activity of the compound in cells. In addition to its antiheparanase activity, SST0001 given in combination with dexamethasone significantly inhibited myeloma tumor growth *in vivo* providing further rationale for incorporation of SST0001 into the clinic.

Materials and Methods

Cell lines and reagents

RPMI-8226, U266, and MPC-11 (all obtained from ATCC); MM.1S and MM.1R (kindly provided by Drs. Nancy Krett and Steven Rosen, Northwestern University). The CAG myeloma cell line was established at the Myeloma Institute for Research and Therapy (Little Rock, AR) as described previously (22). CAG cells were transfected as previously described (23) with empty vector or vector containing the cDNA for human heparanase to generate heparanase low (HPSE-low) and heparanase high (HPSE-high) cells, respectively. During the course of this study the cell lines were confirmed as myeloma cells by their expression of CD138 and kappa immunoglobulin light chain. Cell lines were cultured in RPMI 1640 growth medium supplemented with 10% FBS. SST0001 is a potent inhibitor of heparanase that was produced by chemically modifying porcine mucosal heparin resulting in a molecule that is 100% N-acetylated and 25% glycol split (previously designated ^{100}NA,RO-H, now known as

SST0001, sigma-tau Research Switzerland S.A., Mendrisio, CH; ref. 21).

Heparanase activity assay

Preparation of sulfate-labeled ECM-coated dishes and determination of heparanase enzymatic activity were performed as described in detail elsewhere (24, 25). Briefly, sulfate-labeled ECM coating the surface of 35-mm culture dishes was incubated (4 hours, 37°C, pH 6.0) with constitutively active (GS3) recombinant human heparanase (120 ng/mL) in the absence or presence of the indicated concentration of compound SST0001. The incubation medium containing sulfate-labeled degradation fragments was subjected to gel filtration on a Sepharose CL-6B column. Fractions (0.2 mL) were eluted with PBS and their radioactivity counted in a β-scintillation counter. Degradation fragments of HS side chains were eluted at $0.5 < Kav < 0.8$ (peak II, fractions 15–35). Nearly intact HSPG was eluted just after the Vo ($Kav < 0.2$, peak I, fractions 3–10).

In vivo antitumor activity

Subcutaneous model. A total of 6×10^6 MM.1S or 10×10^6 RPMI-8226 or 1×10^6 MPC-11 or 1×10^6 CAG cells were injected subcutaneously into the left flank of mice. Ten days after the injection of tumor cells, mice were treated with SST0001 for 28 days at doses of 30 mg/kg/day delivered via Alzet osmotic pumps (Durect Corporation) or 120 mg/kg/day (CAG tumors, delivered by distant subcutaneous injection). After 28 days of treatment, animals were euthanized, and the wet weights of tumors recorded. Murine sera were collected before treatment and 2 weeks and 4 weeks after the treatment with SST0001 was begun. Experiments were carried out using 5- to 6-week-old male CB.17 scid/scid or Balb/c mice obtained from Harlan-Sprague Dawley and were housed and monitored in the animal facility at UAB. All experimental procedures and protocols were approved by the Institutional Animal Care and Use Committees of UAB.

Alternatively (studies presented in Fig. 1B), exponentially growing KMS-11 myeloma cells (1.0×10^7/mouse) were injected subcutaneously in the right flank of SCID mice. For RPMI-8226 model, the tumor line was maintained by serial subcutaneous passage of fragments ($3 \times 3 \times 3$ mm) from growing tumors into healthy mice. Each control or drug-treated group included 7 to 8 mice. Treatment started at day 1, when tumors were just palpable. SST0001 was dissolved in saline and delivered twice daily via subcutaneous injections of 60 mg/kg, for 22 to 30 days. Control mice were treated daily in parallel with saline. Growth of the subcutaneous tumor was followed by biweekly measurements of tumor diameters with a Vernier caliper. Tumor weight (TW) was calculated, considering tumor density equal to 1, according to the following formula: tumor weight (mg) = tumor volume (mm^3) = $d^2 \times D/2$, where d and D are the shortest and the longest diameter, respectively. Experiments were carried out using female SCID mice, 8 to 11 weeks old (Charles River). Mice were maintained in laminar flow rooms with constant temperature and humidity. Experimental protocols were approved by the Ethic Committee for Animal Experimentation of the Istituto Nazionale Tumori (Milan, Italy).

SCID-hu model

The SCID-hu model was constructed as previously described (26). Briefly, human fetal femora were cut into halves (approximately $5 \times 5 \times 10$ mm) and implanted subcutaneously into each SCID mouse. At 6 to 8 weeks after implantation of bone, 10^5 CAG HPSE-high cells were injected directly into the marrow cavity of the bone implanted in the SCID-hu host. Twenty days after injection of tumor cells, Alzet osmotic pumps were implanted on the opposite flank of each mouse. Pumps contained either SST0001 (30 mg/kg/day) or saline as a control, and the solution was delivered continuously for 28 days. Murine sera were collected before treatment and 2 weeks and 4 weeks after treatment begun. Animals were also imaged before euthanasia on an IVIS-100 system (Xenogen Corporation). Human immunoglobulin κ light chain levels were measured in murine sera to assess whole animal tumor burden. Sera collected during animal studies were stored at −80°C and analyzed by ELISA (Bethyl Laboratories) in duplicates following manufacturer's protocol.

Combination therapy

A total of 5×10^6 MM.1R cells were injected subcutaneously into the left flank of mice. Ten days after the injection of tumor cells, mice were treated with either saline, SST0001 (60 mg/kg/day via subcutaneous injection), dexamethasone (1 mg/kg/day intraperitoneal) or a combination of SST0001 and dexamethasone for 14 days. After the treatment period, animals were euthanized and the wet weights of tumors recorded.

Immunohistochemistry

Immunohistochemistry was performed on formalin-fixed, paraffin-embedded tissue sections. Briefly, the sections were deparaffinized, dehydrated through a series of graded alcohol washes, followed by antigen retrieval in 10 mmol sodium citrate buffer, pH 6.0. The endogenous peroxidase activity was quenched by incubating the sections in 3% H_2O_2 and blocking nonspecific antigen-binding sites with 5% bovine serum albumin in PBS. The sections were incubated overnight at 4°C with primary antibodies against human VEGF (Neomarkers), human HGF (R&D Systems), mouse CD34 (Hycult Biotechnology), and human MMP-9 (Chemicon). Primary antibody was omitted for negative control. Following incubation with primary antibody, the sections were washed and incubated in appropriate biotin-conjugated secondary antibodies (Vector Laboratories). Vector ABC solution (Vector Laboratories) was added to enhance sensitivity of detection using diaminobenzidine (Vector) and counterstained with hematoxylin. Immunohistochemistry images were taken using a Nikon microscope with a SPOT camera. Microvessel density was measured using the National Institutes of Health ImageJ software.

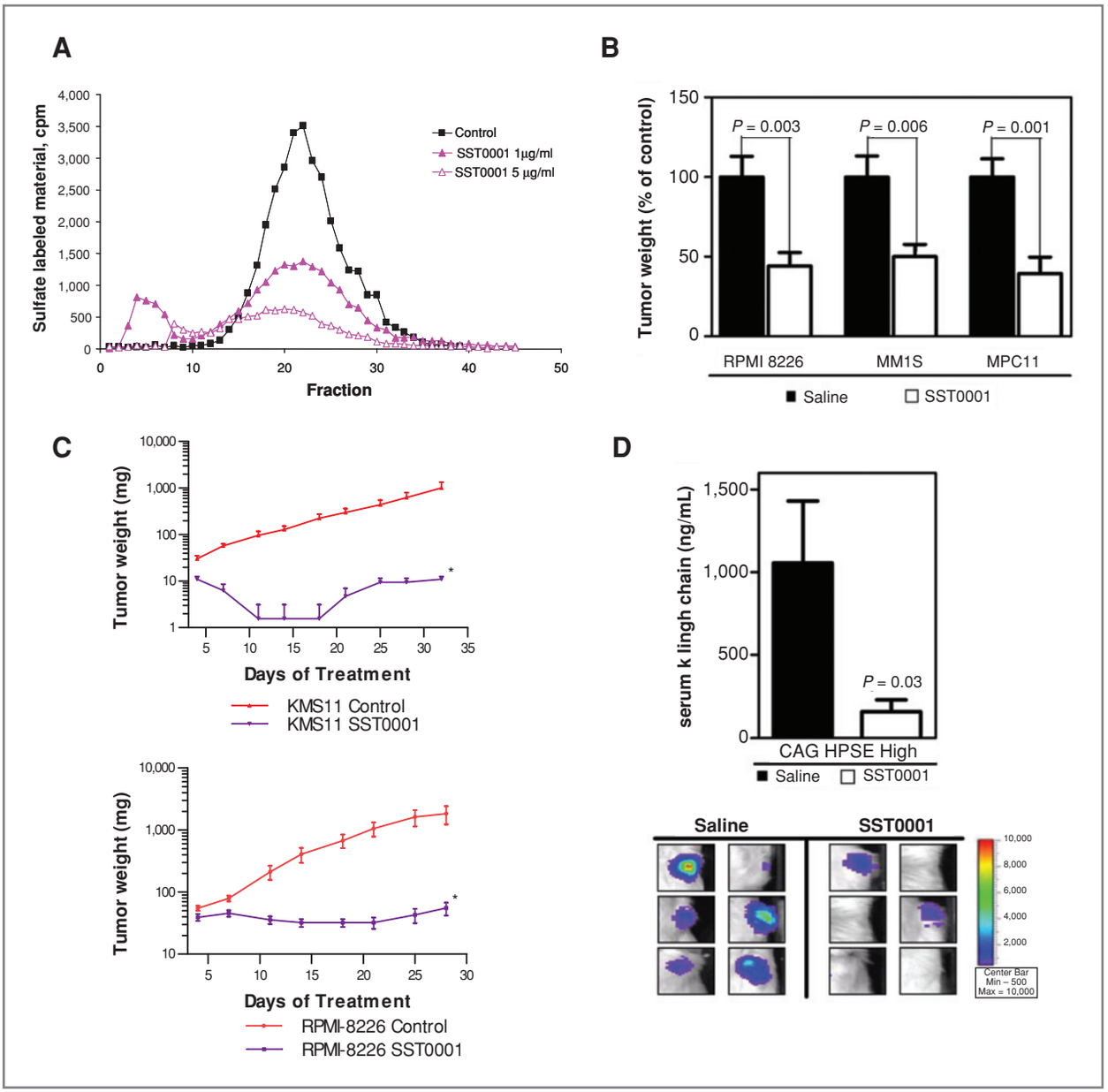

Figure 1. SST0001 is a potent inhibitor of myeloma growth *in vivo.* A, SST0001 inhibits recombinant heparanase-mediated digestion of ^{35}S-labeled heparan sulfate in a dose-dependent manner. B, SST0001 (30 mg/kg/day, 28 days), delivered by Alzet osmotic pumps, inhibited subcutaneous tumor growth in the SCID (RPMI-8226 or MM.1S cells) and syngeneic (MPC-11 cells) models of myeloma. C, growth of KMS-11 (cells injected subcutaneously, top) or RPMI-8226 (tumor fragments implanted subcutaneously, bottom) myeloma tumors was inhibited by twice daily subcutaneous injection of SST0001 (120 mg/kg/day, total daily dose) for 22 to 30 days. *, $P < 0.005$ versus controls, by Student's *t* test. D, quantification of human kappa immunoglobulin light chain in murine sera (top) and bioluminescent imaging (bottom) was used to determine tumor burden in the SCID-hu model of myeloma; mice receiving SST0001 (30 mg/kg/day via Alzet pump) displayed significantly lower tumor burden than control mice as assessed by both measures.

Western blotting

Immunoblot analysis of syndecan-1 (R&D Systems), p-ERK1/2, t-ERK1/2 (Cell Signaling Inc.) was performed as described. Briefly, protein concentration was determined by BCA assay (Pierce) and equal amounts of protein were separated by electrophoresis on 4% to 20% Tris-glycine SDS-PAGE gels (Pierce) and transferred onto either nitrocellulose or Nytran+ membrane. After blocking for 1 hour with TBS containing 0.1% Tween 20 and 5% nonfat dry milk, the blots were exposed to primary antibodies overnight at 4°C, followed by corresponding secondary biotinylated antibodies (Santa Cruz) for 1 hour at room temperature. The proteins were visualized using enhanced chemiluminescence (Amersham Biosciences).

Quantification of VEGF

CAG HPSE-low and HPSE-high cells treated with either PBS or SST0001 (125 μg/mL) were plated at equal density in serum-free RPMI 1640 medium. After 48 hours, conditioned media were collected and the level of VEGF was quantified using ELISA (VEGF; Biosource) following manufacturer's protocol.

Heparanase digestion and shedding of syndecan-1

Recombinant human heparanase was incubated with partially purified syndecan-1 in the presence or absence of SST0001 for 24 hours at 37°C in heparanase activity buffer containing 50 mmol/L NaCl, 1 mmol/L DTT, 1 mmol/L $CaCl_2$, and 10 mmol/L phosphate citrate buffer, pH 6.0. The effect of SST0001 on inhibition of syndecan-1 heparan sulfate digestion by heparanase was then assessed by immunoblot analysis. To determine the effects of SST0001 treatment on syndecan-1 shedding, medium conditioned for 24 hours by CAG HPSE-low and HPSE-high cells treated with either PBS or SST0001 was collected, and the levels of shed syndecan-1 present in the conditioned medium was determined by ELISA as described (23).

Gelatin zymography

To determine levels of active MMP-9, conditioned media from CAG HPSE-low and HPSE-high cells treated with either PBS or SST0001 was subjected to gelatin zymography as previously described (27). Briefly, equal numbers of cells were plated in serum-free media for 48 hours. Media was collected, concentrated using Spin-X UF 30-kD cutoff concentrators (Corning) and equal protein was mixed with nonreducing sample buffer and analyzed by SDS-PAGE using 10% polyacrylamide gels copolymerized with gelatin following manufacturer's protocol (BioRad). Sites of proteolytic activity were visualized as clear bands against the blue background of Coomassie stained gelatin.

Statistical analysis

Experiments were repeated a minimum of 3 times. Comparisons were analyzed by Student *t* test or 1-way ANOVA using GraphPad Prism. *P* values less than 0.05 were considered statistically significant. For combination therapy studies, the effect of drug combination was determined using the GLM procedure. All data are mean ± SEM.

Results

SST0001 is a potent inhibitor of myeloma growth *in vivo*

SST0001 (^{100}NA,RO-H) has been previously shown to significantly inhibit heparanase-mediated extracellular matrix degradation in a cell-free assay (21). In limited studies, we and others have reported that SST0001 inhibits the *in vivo* subcutaneous growth of CAG myeloma cells (28), the experimental metastasis of B16-BL6 melanoma cells (29), and more recently, a xenograft model of Ewing's sarcoma (30). To further validate SST0001 as a potential myeloma therapeutic we first examined the antiheparanase activity of SST0001 (Fig. 1A) and then tested the efficacy of SST0001 against growth of several myeloma cell lines. Using a well established heparanase activity assay, we measured the heparanase inhibitory activity of SST0001 against recombinant human heparanase. Results from this assay further confirm that SST0001 is a potent inhibitor of heparanase enzymatic activity in a cell-free model. Based on these results we then examined the antitumor activity of SST0001, using 2 different *in vivo* models (human MM.1S and RPMI-8226 cell lines in SCID mice and the murine MPC-11 cell line in syngeneic Balb/c mice). Ten days after injection of myeloma cells, mice bearing established subcutaneous tumors were treated for 28 days with SST0001 (30 mg/kg/day delivered by Alzet pump). This resulted in significant inhibition of myeloma tumor growth. Average weights of MM.1S, RPMI-8226, and MPC-11 tumors were reduced 50%, 56%, and 61%, respectively, as compared with controls (Fig. 1B). In a separate line of experiments, KMS-11 cells or actively growing RPMI-8226 tumor fragments were passaged subcutaneously into tumor-free animals. Treatment began on day 1, when tumors were just palpable. In contrast to delivery by Alzet pump, in these experiments, SST0001 was delivered by subcutaneous injection of 60 mg/kg of the compound, twice a day. Treatment of mice bearing KMS-11 and RPMI 8226 tumors resulted in nearly complete inhibition of tumor growth (98% and 99%, respectively) as compared with controls (Fig. 1C).

To more rigorously examine the therapeutic utility of SST0001 we employed the SCID-hu animal model. This model facilitates growth of myeloma tumors within the human bone marrow, thus accurately mimicking the human disease (26). CAG human myeloma cells expressing high levels of heparanase (HPSE-high cells) were injected directly into human bones engrafted in SCID mice. The tumors were allowed to establish and grow for 20 days, followed by treatment of the tumor-bearing mice for 28 days with saline or SST0001 (30 mg/kg/day delivered by Alzet pump). SST0001 significantly inhibited the growth of HPSE-high tumors within the bone as determined by bioluminescent imaging (Fig. 1D, bottom) and quantification of levels of human immunoglobulin κ light-chain present within the serum of tumor-bearing mice (Fig. 1D, top). We did not observe any adverse side effect in any of these *in vivo* animal models, even at doses as high as 120 mg/kg/day. Pathological evaluation of liver, lung spleen, and kidney of SST0001-treated mice displayed no altered morphology as compared with mice treated with saline, indicating no adverse toxicities. These data demonstrate that SST0001 is a potent inhibitor of myeloma growth *in vivo* and the antitumor effect of SST0001 is not cell line specific.

SST0001 inhibits angiogenesis *in vivo*

Heparanase is known to enhance angiogenesis and we previously reported that high levels of heparanase correlate with an increase in bone marrow microvessel density (MVD) in myeloma patients and in animal models of

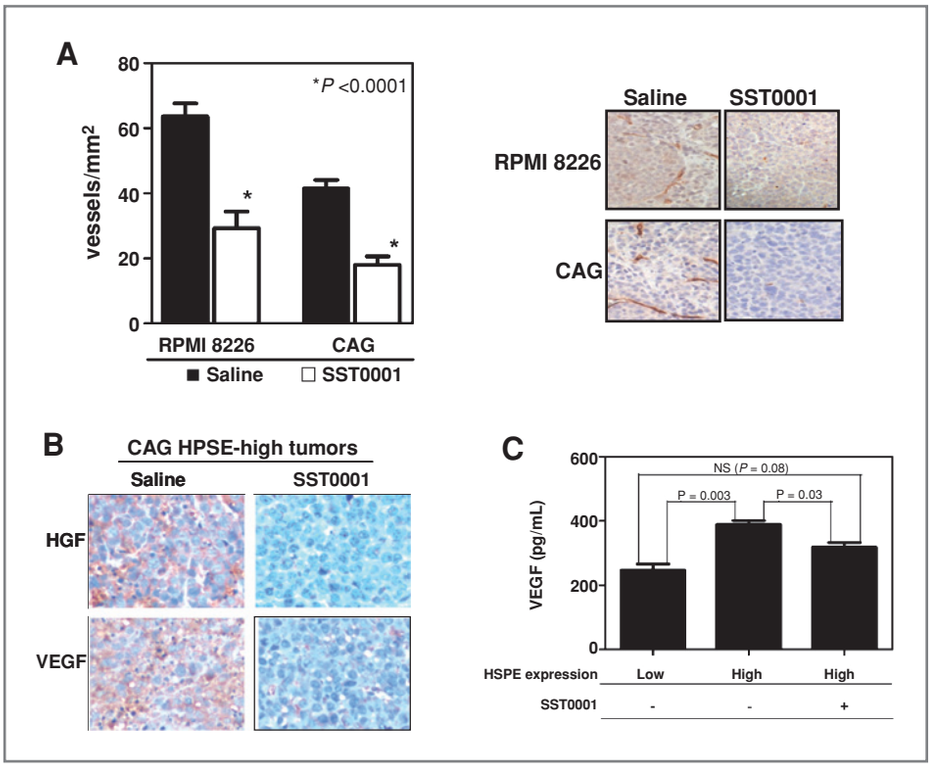

Figure 2. SST0001 inhibits angiogenesis and HGF and VEGF expression *in vivo*. A, SCID mice bearing subcutaneous myeloma tumors formed by RPMI-8226 and CAG cells treated with SST0001 or saline for 28 days. After treatment, microvessel density was quantified (left) in sections of the tumor tissue using anti-CD34 immunohistochemical analysis (representative images, right). SST0001 significantly inhibited tumor vascularity. B, mice bearing subcutaneous tumors formed by HPSE-high cells were treated with either saline or SST0001 (30 mg/kg/day, delivered by Alzet osmotic pumps) for 28 days. Following euthanasia of animals, the tumors were removed and subjected to immunohistochemical analysis of HGF and VEGF. In tumors from animals treated with SST0001, the intratumoral levels of both HGF and VEGF were reduced dramatically as compared with animals treated with saline. C, levels of VEGF in the conditioned medium from HPSE-low or HPSE-high CAG cells treated with saline or 125 μg/mL SST0001 (6.75 μmol/L) were measured by ELISA. SST0001 treatment significantly decreased the accumulation of VEGF in HPSE-high cells ($n = 3$ for each group).

myeloma (5). Therefore, to determine if the heparanase inhibitor SST0001 was interfering with tumor angiogenesis, we measured the MVD in tumors derived from wild-type CAG and RPMI-8226 myeloma cells, using anti-CD34 immunohistochemistry, a surrogate marker of angiogenesis in myeloma (31). Treatment of animals with SST0001 significantly reduced the numbers of $CD34^+$ vessels in these tumors as compared with control animals treated with saline (Fig. 2A). We have recently discovered that in myeloma cells, heparanase enhances expression and secretion of HGF (32) and VEGF (33), 2 factors important for myeloma growth and angiogenesis (34, 35). Therefore, we assessed whether treatment of tumor-bearing animals with SST0001 would inhibit expression of HGF and VEGF and contribute to inhibition of tumor growth and angiogenesis. Immunohistochemical analysis revealed a dramatic decrease in the intra-tumoral levels of both HGF and VEGF in HPSE-high tumors treated with SST0001 as compared with saline-treated controls (Fig. 2B). This reduced level of HGF and VEGF was paralleled by diminished microvessel density in the SST0001-treated animals as compared with controls (5.9 vessels/mm^2 vs. 40.3 vessels/mm^2, respectively). Moreover, treatment of HPSE-high cells *in vitro* with SST0001 resulted in a significant reduction in the level of VEGF secreted into the medium (Fig. 2C). These results point to a novel mechanism of action for SST0001 whereby it blocks heparanase activity leading to diminished HGF and VEGF production, 2 factors modulated by heparanase, and inhibition of myeloma growth and angiogenesis.

Disruption of the heparanase/syndecan-1 axis in myeloma by SST0001

Therapeutic targeting of the heparanase/syndecan-1 axis, which drives an aggressive myeloma phenotype through regulation of multiple pathways, represents a unique opportunity to strategically inhibit myeloma growth (6). SST0001 has been previously identified as an inhibitor of heparanase enzymatic activity in cell-free assays (21); however, the ability of SST0001 to inhibit heparanase activity in a tumor cell has not been demonstrated. To better establish the therapeutic potential and provide insight into the mechanism of action of this compound, we examined whether treatment of cells making high levels of heparanase with SST0001 would affect the size of the

syndecan-1 heparan sulfate proteoglycan being expressed by those cells. Syndecan-1, the predominant heparan sulfate proteoglycan on myeloma cells, (36, 37) runs as a broad smear when analyzed by Western blotting due to the molecular heterogeneity in the size and number of heparan sulfate chains attached to the syndecan-1 core protein. When heparanase levels are elevated in the CAG cells (HPSE-high cells), syndecan-1 resolves as a lower molecular weight smear than those in control cells due to clipping of the heparan sulfate chains by the heparanase enzyme (23). Therefore, we hypothesized that treatment of HPSE-high cells with SST0001 would inhibit heparanase activity leading to a higher molecular weight form of syndecan-1. To test this in a cell-free system, partially purified syndecan-1 was incubated with recombinant heparanase in the presence of SST0001 in a buffer that promotes heparanase activity. Western blotting for syndecan-1 revealed that SST0001 inhibited heparanase digestion of heparan sulfate as reflected by the high molecular weight smear as compared with syndecan-1 digested with heparanase in the absence of SST0001 (Fig. 3A). Next, we treated HPSE-high cells with SST0001 for 24 hours and then assessed the molecular weight of syndecan-1 to determine if SST0001 was able to inhibit heparanase activity in those cells. Western blotting of cell extracts revealed that as the concentration of SST0001 was increased, the molecular size of the syndecan-1 smear increased thus indicating that SST001 effectively blocked the cellular heparanase enzyme activity (Fig. 3B).

Heparanase enzyme activity upregulates expression of MMP-9, which cleaves syndecan-1 causing its shedding from the cell surface (27); this shed syndecan-1 promotes angiogenesis, growth, and metastasis of myeloma tumors (7, 23). To determine if shed syndecan-1 was diminished by treating cells with SST0001, we quantified by ELISA the amount of shed syndecan-1 in conditioned medium from HPSE-high cells treated with saline or SST0001. Treatment with SST0001 significantly reduced the amount of shed syndecan-1 in the conditioned medium of HPSE-high cells as compared with saline-treated HPSE-high cells (Fig. 3C). Western blotting of shed syndecan-1 in conditioned medium further confirmed that SST0001 diminished shedding of syndecan-1 and inhibited heparanase digestion of heparan sulfate as indicated by the loss of the lower

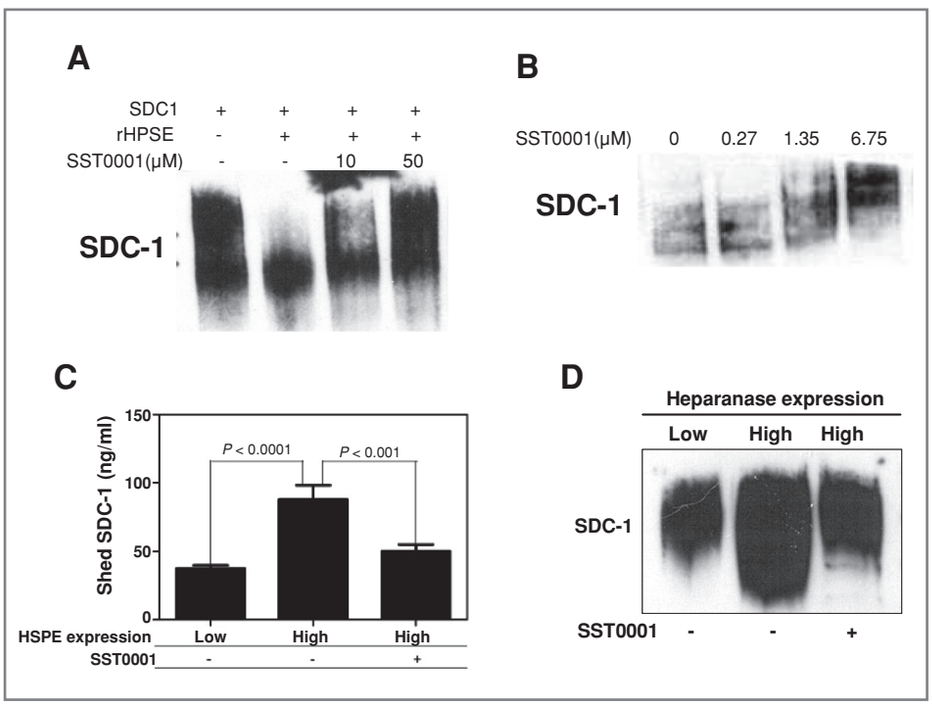

Figure 3. SST0001 inhibits heparanase activity in tumor cells expressing high levels of the enzyme. A, in a cell-free system, SST0001 blocked heparanase-mediated digestion of the heparan sulfate chains of partially purified syndecan-1(SDC1). The proteoglycan was incubated with recombinant heparanase (rHPSE) in the presence or absence of SST0001 followed by Western blotting. Note that in the presence of SST0001, the molecular size of syndecan-1 is larger than in the absence of the inhibitor. B, HPSE-high cells were treated overnight with increasing concentration of SST0001; the cells were extracted and analyzed by Western blotting. SST0001 inhibited heparanase digestion of the heparan sulfate chains of syndecan-1, resulting in the high molecular weight form of syndecan-1. C, the amount of syndecan-1 shed into the conditioned medium of HPSE-low or HPSE-high cells treated with SST0001 (125 μg/mL; 6.75 μmol/L) or saline was quantified by ELISA. SST0001 significantly inhibited shedding of syndecan-1 from HPSE-high cells ($n = 3$ for each group). D, conditioned medium from HPSE-low cells or HPSE-high cells treated with SST0001 (6.75 μmol/L) or saline was subjected to Western blot analysis of syndecan-1. Results confirm that levels of shed syndecan-1 are reduced following treatment of HPSE-high cells with SST0001. Note also that the molecular size of shed syndecan-1 in conditioned medium from HPSE-high cells treated with SST0001 is also larger than that found in untreated cells, again confirming the ability of the compound to block the activity of heparanase.

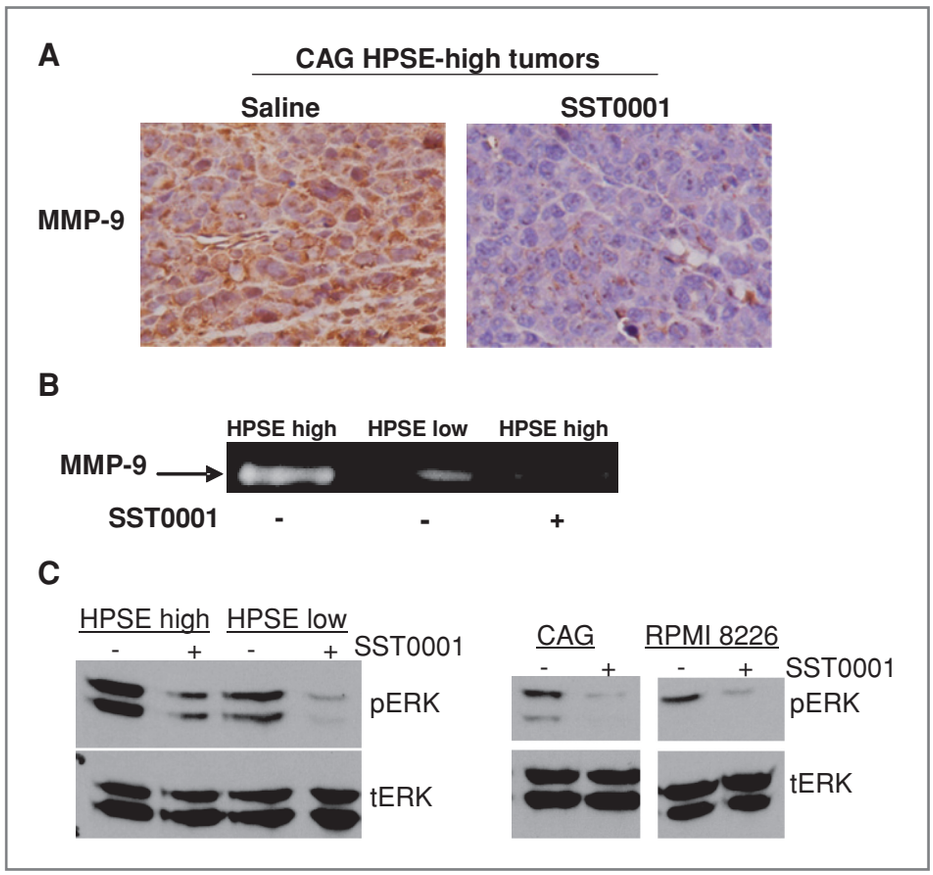

Figure 4. SST0001 blocks heparanase-mediated MMP-9 expression and ERK signaling. A, mice bearing tumors formed by HPSE-high cells injected subcutaneously were treated with SST0001 or saline. Tumors were excised and immunohistochemical analysis for MMP-9 revealed diminished levels of expression within SST0001-treated tumors as compared with tumors from animals treated with saline. B, conditioned media from HPSE-low cells or HPSE-high cells treated with SST0001 (125 μg/mL; 6.75 μmol/L) or saline were subjected to gelatin zymography. HPSE-high cells treated with SST0001 had significantly reduced levels of MMP-9 activity in their medium as compared with cells treated with saline. C, ERK signaling was assessed by Western blotting of extracts from myeloma cell lines treated with SST0001 or saline. Heparanase inhibition with SST0001 caused a dose-dependent reduction in phospho-ERK (pERK) signaling.

molecular weight portion of the syndecan-1 smear (Fig. 3D).

Because of the link between MMP-9 expression and syndecan-1 shedding (27), we assessed levels of MMP-9 expression in tumors formed by HPSE-high cells. Results demonstrate markedly reduced MMP-9 expression in SST0001-treated tumor as compared with control tumors (Fig. 4A). In addition, treatment of cells with SST0001 *in vitro* revealed that MMP-9 proteolytic activity is diminished (Fig. 4B). In myeloma cells, heparanase stimulates MMP-9 expression through activation of the ERK 1/2 MAPK pathway (27). Treatment of CAG HPSE-high and HPSE-low cells as well as wild-type CAG and RPMI-8226 cells (all of which express heparanase at detectable levels) with SST0001 *in vitro* resulted in a dose-dependent reduction in ERK phosphorylation (Fig. 4C). These findings further illustrate that SST0001 impacts the downstream targets of heparanase activity on tumor cells *in vitro* and *in vivo*.

SST0001 in combination with dexamethasone potently inhibits myeloma growth *in vivo*

The emergence of novel myeloma therapeutics (e.g., bortezomib, thalidomide) that function through pathways different than conventional cytotoxic drugs, has greatly impacted myeloma therapy (38). Recent clinical studies have demonstrated that these drugs can significantly improve therapeutic outcomes when combined with common myeloma drugs such as dexamethasone and other cytotoxic agents (39). Therefore, we sought to determine if SST0001, which acts by inhibiting heparanase and appears to target the tumor microenvironment, would be effective when used in combination with other drugs used to treat myeloma patients. In pilot experiments, we tested SST0001 in combination with several common myeloma agents including dexamethasone, doxorubicin, and bortezomib. Although all 3 combinations provided favorable results, the combination of dexamethasone with SST0001 was most effective (data not shown). Therefore, we chose this combination for analysis *in vivo*. SST0001 and dexamethasone combination therapy was tested against subcutaneous myeloma tumor growth in SCID mice (using human MM.1R myeloma cells) and in Balb/c mice (using murine MPC-11 myeloma cells), thereby representing drug-resistant and immuno-competent models of myeloma, respectively. In both settings, the combination therapy significantly inhibited tumor growth more effectively than single agent therapy alone. In the drug-resistant MM.1R model, combination therapy inhibited tumor growth by 80% when compared with saline-treated

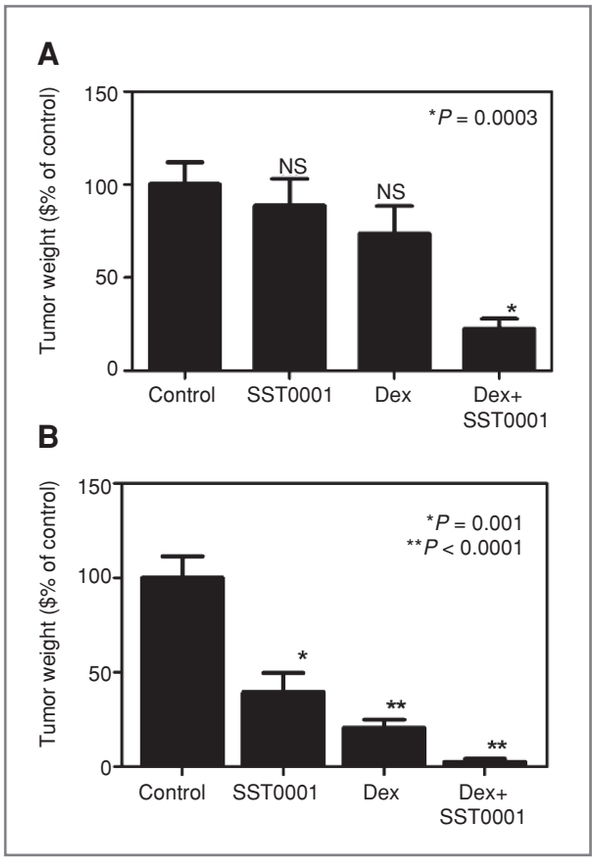

Figure 5. SST0001 in combination with dexamethasone is a potent inhibitor of myeloma tumor growth *in vivo*. A, dexamethasone-resistant MM.1R tumors were established subcutaneously in SCID mice and mice were injected with either saline, a low dose of SST0001 (60 mg/kg/day, as compared with 120 mg/kg/day used for studies in Fig. 1B), dexamethasone (1 mg/kg/day), or SST0001 + dexamethasone for 14 days. Mice receiving combination therapy had significantly smaller tumors compared with control mice ($n = 8$ for each group). B, murine MPC-11 tumors were established in syngeneic BALB/c mice. Mice were then treated with either saline, SST0001 (60 mg/kg/day), dexamethasone (1 mg/kg/day), or SST0001 + dexamethasone for 14 days. At the doses utilized, combination therapy potently inhibited tumor growth and was significantly more effective than single agent therapies when compared with saline-treated controls ($n = 6$–10 for each group). In both experiments, the effect of the drug combination was additive as determined using the GLM procedure.

controls, whereas, dexamethasone and SST0001 single agent therapy modestly inhibited tumor growth, 26% and 12%, respectively (Fig. 5A). In the syngeneic model, combination therapy inhibited tumor growth 97% when compared with saline-treated controls, whereas, dexamethasone and SST0001 single agent therapy only resulted in 80% and 61% inhibition of tumor growth, respectively (Fig. 5B). In both cases, assessment of the combination of SST0001 and dexamethasone revealed an additive effect in inhibiting myeloma tumor growth; warranting more in-depth experiments to fully assess the potential of SST0001 as part of a combination therapy regimen.

Discussion

The present study demonstrates that the heparanase inhibitor SST0001 disrupts the myeloma tumor microenvironment resulting in diminished tumor growth. The compound was highly efficacious against human myeloma tumors growing in mice, including tumors that were established and growing within human bones. Pharmacodynamic studies demonstrated that SST0001 effectively targets heparanase and its downstream effects *in vivo* including inhibition of tumor angiogenesis, reduction in levels of HGF, VEGF, and MMP-9 and diminished shedding of syndecan-1 (Fig 6). Together these effects of SST0001 dramatically blunt the normally aggressive phenotype of myeloma driven by the heparanase/syndecan-1 axis thus establishing the potential of this compound for myeloma therapy.

The results also indicate that SST0001 effectively blocked activity of the target enzyme. The antiheparanase activity of SST0001 was originally determined using an assay that measures heparanase-mediated release of radiolabeled heparan sulfate from extracellular matrix (21). However, this assay does not assess the ability of SST0001 to block heparanase activity in living cells. We assessed the anti-heparanase activity of SST0001 on myeloma cells by examining the size of the heparan sulfate proteoglycan syndecan-1 from cells grown in the presence or absence of SST0001 and found that in the presence of the inhibitor,

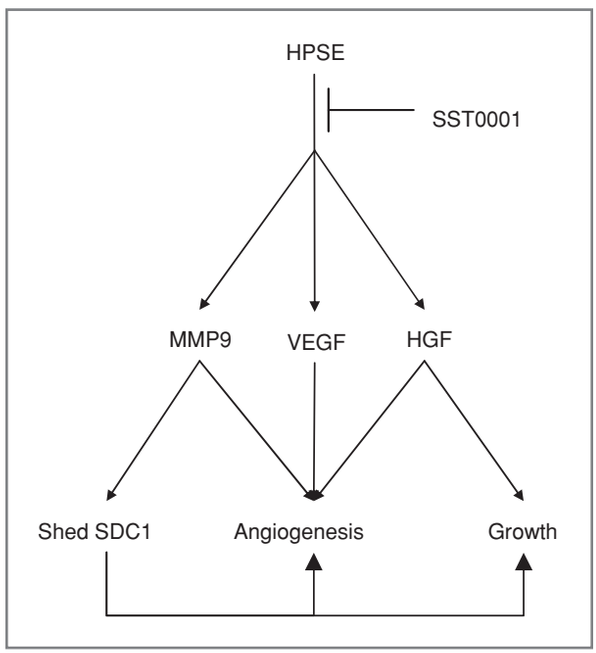

Figure 6. SST0001 inhibits heparanase and its downstream effectors to block myeloma growth and angiogenesis. Heparanase activity enhances expression of VEGF, HGF, and MMP-9 and stimulates shedding of syndecan-1, thereby fueling an aggressive myeloma phenotype. Through inhibition of enzyme activity, SST0001 shuts down these multiple pathways that together stimulate myeloma tumor growth.

the molecular size of syndecan-1 was higher than that in untreated cells. This result demonstrates that trimming of heparan sulfate by heparanase produced by the cells was blocked by SST0001 thus indicating that heparanase activity was inhibited.

The downstream effects of heparanase including enhanced angiogenesis, growth factor levels, and shed syndecan-1 (5, 23, 27, 33), were all diminished following treatment with SST0001, effects that were likely due to the enzyme inhibitory activity of the compound. Heparanase has been closely associated with increased tumor angiogenesis in a number of cancers (4). We previously demonstrated that myeloma patients with high heparanase enzyme activity within their tumors exhibit enhanced angiogenesis as compared with patients with low levels of enzyme activity (5). This study also demonstrated a relationship between heparanase and myeloma angiogenesis in animal models of myeloma. Thus, observation in the present work that SST0001 inhibits angiogenesis is entirely consistent with it being an inhibitor of heparanase. Moreover, the mechanism behind the reduction in angiogenesis in tumors from animals treated with SST0001 is likely driven, at least in part, by reduced levels of HGF, VEGF, and MMP-9, all factors that are known to contribute to the angiogenic phenotype of myeloma (35, 40). Heparanase is known to upregulate VEGF expression in HEK293, MDA-MB-435 breast carcinoma, and rat C6 glioma cells as well as in myeloma cells (33, 41). HGF working in concert with syndecan-1 has also been shown to be critical for myeloma growth and angiogenesis, as circulating and bone marrow levels of HGF are significantly elevated in myeloma patients and the blood levels of HGF correlate with bone marrow MVD (34, 42–44).

MMP-9 can also contribute to angiogenesis by promoting the release of VEGF from tumor cells (45). Although relatively little is known about the role of MMP-9 in myeloma, our lab discovered that MMP-9 expression is upregulated by heparanase and that MMP-9 increases shedding of syndecan-1 from the surface of myeloma cells (27). Our finding that treatment of animals with SST0001 diminishes intratumoral levels of MMP-9 and that this results in decreased cellular syndecan-1 shedding also points to SST0001 as a potent *in vivo* inhibitor of heparanase.

Disruption of the heparanase/syndecan-1 axis by SST0001 with reduction in syndecan-1 shedding likely has multiple effects on tumor progression. For example, high levels of shed syndecan-1 correlate with poor prognosis in myeloma patients (9), and when shed syndecan-1 is increased in animal models of myeloma, tumor growth, metastasis, and progression are dramatically enhanced (46). Once shed into the microenvironment, syndecan-1 can complex with heparin-binding growth factors, such as FGF2 (47), HGF (48), and VEGF (33), and serves to present these growth factors to their receptors, leading to enhanced myeloma growth and angiogenesis. Alternatively, through its core protein, syndecan-1 can promote integrin activation and drive angiogenesis (49). In myeloma, shed syndecan-1 stimulates angiogenesis, in part, by participating in activation of the αvβ3 integrin (33). The critical role of syndecan-1 in supporting myeloma growth *in vivo* has recently been confirmed by knockdown of expression of either syndecan-1 or heparan sulfate (50, 51). Thus, the effect of SST0001 on inhibiting syndecan-1 shedding may contribute significantly to its antitumor effects.

Although use of SST0001 as a single agent effectively dampened tumor growth, the combination of dexamethasone and SST0001 was much more potent. Because we showed that this combination was effective against a dexamethasone-resistant cell line (MM.1R), it is possible that SST0001 may help overcome tumor resistance to dexamethasone and other chemotherapeutic agents. In addition, inclusion of SST0001 to a therapeutic regimen might facilitate lowering the dose of chemotherapeutic drugs thereby lessening the side-effects of treatment.

The data presented here confirms that SST0001, a modified nonanticoagulant heparin, is an effective heparanase inhibitor *in vivo* against myeloma exhibiting no obvious side effects at the concentrations used in this study. Its strong effect as an antiangiogenic agent and its ability to diminish shedding of syndecan-1 demonstrate that SST0001 has dramatic impact on the myeloma microenvironment resulting in diminished tumor progression. SST0001 is now completing its preclinical development with the objective to enter into clinical testing soon. These further investigations of SST0001 and similar compounds will determine their potential as therapeutic agents against myeloma and other heparanase-expressing cancers.

Disclosure of Potential Conflicts of Interest

R. D. Sanderson, G. Torri, I. Vlodavsky, and F. Zunino received research funding from sigma-tau Research Switzerland; S. Penco, C. Pisano, and P. Carminati are employees of sigma-tau Industrie Farmaceutiche Riunite S.p.A; A. Naggi, G. Torri, B. Casu, S. Penco, C. Pisano, and P. Carminati are listed as inventors on a patent for SST0001. J. P. Ritchie, V. C. Ramani, Y. Ren, M. Tortoreto, and Y. Yang declare no conflict of interest.

Acknowledgments

Histology services were performed by the UAB Center for Metabolic Bone Disease's Histomorphometry and Molecular Analysis Core and animal imaging studies were performed by the Small Animal Imaging Core of the UAB Comprehensive Cancer Center. We thank Dr. Renee A. Desmond (UAB Comprehensive Cancer Center) for providing assistance with statistical analysis.

Grant Support

NIH grants CA138535 (R. D. Sanderson), CA135075 (R. D. Sanderson), and CA106456 (I. Vlodavsky), UAB Center for Metabolic Bone Disease NIH Institutional Predoctoral Training Grant T32-AR047512 (J. P. Ritchie), Multiple Myeloma Research Foundation (MMRF) Senior Investigator Award (Y. Yang), MMRF Research Fellow Award (V.P. Ramani), the UAB Small Animal Imaging Shared Facility (NIH P30CA013148), and by research contracts from sigma-tau Research Switzerland S.A., Mendrisio, CH (R. D. Sanderson, F. Zunino, G. Torri, I. Vlodavsky).

The costs of publication of this article were defrayed in part by the payment of page charges. This article must therefore be hereby marked *advertisement* in accordance with 18 U.S.C. Section 1734 solely to indicate this fact.

Received September 15, 2010; revised November 19, 2010; accepted December 17, 2010; published OnlineFirst January 21, 2011.

References

1. Bergsagel D. The incidence and epidemiology of plasma cell neoplasms. Stem Cells 1995;13Suppl 2:1–9.
2. Laubach JP, Richardson PG, Anderson KC. The evolution and impact of therapy in multiple myeloma. Med Oncol;27 Suppl 1:S1–6.
3. Anderson KC. Targeted therapy of multiple myeloma based upon tumor-microenvironmental interactions. Exp Hematol 2007;35:155–62.
4. Barash U, Cohen-Kaplan V, Dowek I, Sanderson RD, Ilan N, Vlodavsky I. Proteoglycans in health and disease: new concepts for heparanase function in tumor progression and metastasis. FEBS J 2010;277: 3890–903.
5. Kelly T, Miao HQ, Yang Y, Navarro E, Kussie P, Huang Y, et al. High heparanase activity in multiple myeloma is associated with elevated microvessel density. Cancer Res 2003;63:8749–56.
6. Sanderson RD, Yang Y, Kelly T, MacLeod V, Dai Y, Theus A. Enzymatic remodeling of heparan sulfate proteoglycans within the tumor microenvironment: growth regulation and the prospect of new cancer therapies. J Cell Biochem 2005;96:897–905.
7. Sanderson RD, Yang Y. Syndecan-1: a dynamic regulator of the myeloma microenvironment. Clin Exp Metastasis 2008;25:149–59.
8. Sanderson RD, Yang Y, Suva LJ, Kelly T. Heparan sulfate proteoglycans and heparanase–partners in osteolytic tumor growth and metastasis. Matrix Biol 2004;23:341–52.
9. Mahtouk K, Hose D, Raynaud P, Hundemer M, Jourdan M, Jourdan E, et al. Heparanase influences expression and shedding of syndecan-1, and its expression by the bone marrow environment is a bad prognostic factor in multiple myeloma. Blood 2007;109:4914–23.
10. McKenzie EA. Heparanase: a target for drug discovery in cancer and inflammation. Br J Pharmacol 2007;151:1–14.
11. Karoli T, Liu L, Fairweather JK, Hammond E, Li CP, Cochran S, et al. Synthesis, biological activity, and preliminary pharmacokinetic evaluation of analogues of a phosphosulfomannan angiogenesis inhibitor (PI-88). J Med Chem 2005;48:8229–36.
12. Khasraw M, Pavlakis N, McCowatt S, Underhill C, Begbie S, de Souza P, et al. Multicentre phase I/II study of PI-88, a heparanase inhibitor in combination with docetaxel in patients with metastatic castrate-resistant prostate cancer. Ann Oncol 2010;21:1302–7.
13. Khachigian LM, Parish CR. Phosphomannopentaose sulfate (PI-88): heparan sulfate mimetic with clinical potential in multiple vascular pathologies. Cardiovasc Drug Rev 2004;22:1–6.
14. Bar-Ner M, Eldor A, Wasserman L, Matzner Y, Cohen IR, Fuks Z, et al. Inhibition of heparanase-mediated degradation of extracellular matrix heparan sulfate by non-anticoagulant heparin species. Blood 1987;70:551–7.
15. Lazo-Langner A, Goss GD, Spaans JN, Rodger MA. The effect of low-molecular-weight heparin on cancer survival. A systematic review and meta-analysis of randomized trials. J Thromb Haemost 2007;5:729–37.
16. Casu B, Vlodavsky I, Sanderson RD. Non-anticoagulant heparins and inhibition of cancer. Pathophysiol Haemost Thromb 2008;36:195–203.
17. Zangari M, Barlogie B, Cavallo F, Bolejack V, Fink L, Tricot G. Effect on survival of treatment-associated venous thromboembolism in newly diagnosed multiple myeloma patients. Blood Coagul Fibrinolysis 2007;18:595–8.
18. Mitsiades CS, Rouleau C, Echart C, Menon K, Teicher B, Distaso M, et al. Preclinical studies in support of defibrotide for the treatment of multiple myeloma and other neoplasias. Clin Cancer Res 2009;15: 1210–21.
19. Vlodavsky I, Mohsen M, Lider O, Svahn CM, Ekre HP, Vigoda M, et al. Inhibition of tumor metastasis by heparanase inhibiting species of heparin. Invasion Metastasis 1994;14:290–302.
20. Casu B, Guerrini M, Naggi A, Perez M, Torri G, Ribatti D, et al. Short heparin sequences spaced by glycol-split uronate residues are antagonists of fibroblast growth factor 2 and angiogenesis inhibitors. Biochemistry 2002;41:10519–28.
21. Naggi A, Casu B, Perez M, Torri G, Cassinelli G, Penco S, et al. Modulation of the heparanase-inhibiting activity of heparin through selective desulfation, graded N-acetylation, and glycol splitting. J Biol Chem 2005;280:12103–13.
22. Borset M, Hjertner O, Yaccoby S, Epstein J, Sanderson RD. Syndecan-1 is targeted to the uropods of polarized myeloma cells where it promotes adhesion and sequesters heparin-binding proteins. Blood 2000;96:2528–36.
23. Yang Y, Macleod V, Miao HQ, Theus A, Zhan F, Shaughnessy JD Jr, et al. Heparanase enhances syndecan-1 shedding: A novel mechanism for stimulation of tumor growth and metastasis. J Biol Chem 2007;282:13326–33.
24. Vlodavsky I, Fuks Z, Bar-Ner M, Ariav Y, Schirrmacher V. Lymphoma cell-mediated degradation of sulfated proteoglycans in the subendothelial extracellular matrix: relationship to tumor cell metastasis. Cancer Res 1983;43:2704–11.
25. Vlodavsky I. Preparation of extracellular matrices produced by cultured corneal endothelial and PF-HR9 endodermal cells. Curr Protoc Cell Biol 2001;Chapter 10:Unit 10.4.
26. Yaccoby S, Barlogie B, Epstein J. Primary myeloma cells growing in SCID-hu mice: a model for studying the biology and treatment of myeloma and its manifestations. Blood 1998;92:2908–13.
27. Purushothaman A, Chen L, Yang Y, Sanderson RD. Heparanase stimulation of protease expression implicates it as a master regulator of the aggressive tumor phenotype in myeloma. J Biol Chem 2008;283:32628–36.
28. Yang Y, MacLeod V, Dai Y, Khotskaya-Sample Y, Shriver Z, Venkataraman G, et al. The syndecan-1 heparan sulfate proteoglycan is a viable target for myeloma therapy. Blood 2007;110:2041–8.
29. Hostettler N, Naggi A, Torri G, Ishai-Michaeli R, Casu B, Vlodavsky I, et al. P-selectin- and heparanase-dependent antimetastatic activity of non-anticoagulant heparins. Faseb J 2007;21:3562–72.
30. Shafat I, Ben-Arush MW, Issakov J, Meller I, Naroditsky I, Tortoteto M, et al. Preclinical and clinical significance of heparanase in Ewing's sarcoma. J Cell Mol Med 2010. Epub ahead of print.
31. Pruneri G, Ponzoni M, Ferreri AJ, Decarli N, Tresoldi M, Raggi F, et al. Microvessel density, a surrogate marker of angiogenesis, is significantly related to survival in multiple myeloma patients. Br J Haematol 2002;118:817–20.
32. Ramani VC, Yang Y, Ren Y, Nan L, Sanderson RD. Heparanase plays a dual role in driving hepatocyte growth factor (HGF) signaling by enhancing HGF expression and activity. J Biol Chem. In press 2011.
33. Purushothaman A, Uyama T, Kobayashi F, Yamada S, Sugahara K, Rapraeger AC, et al. Heparanase-enhanced shedding of syndecan-1 by myeloma cells promotes endothelial invasion and angiogenesis. Blood 2010;115:2449–57.
34. Borset M, Seidel C, Hjorth-Hansen H, Waage A, Sundan A. The role of hepatocyte growth factor and its receptor c-Met in multiple myeloma and other blood malignancies. Leuk Lymphoma 1999;32:249–56.
35. Jakob C, Sterz J, Zavrski I, Heider U, Kleeberg L, Fleissner C, et al. Angiogenesis in multiple myeloma. Eur J Cancer 2006;42:1581–90.
36. Sanderson RD, Sneed TB, Young LA, Sullivan GL, Lander AD. Adhesion of B lymphoid (MPC-11) cells to type I collagen is mediated by the integral membrane proteoglycan, syndecan. J Immunol 1992;148: 3902–11.
37. Ridley RC, Xiao H, Hata H, Woodliff J, Epstein J, Sanderson RD. Expression of syndecan regulates human myeloma plasma cell adhesion to type I collagen. Blood 1993;81:767–74.
38. Kumar SK, Rajkumar SV, Dispenzieri A, Lacy MQ, Hayman SR, Buadi FK, et al. Improved survival in multiple myeloma and the impact of novel therapies. Blood 2008;111:2516–20.
39. Lonial S, Cavenagh J. Emerging combination treatment strategies containing novel agents in newly diagnosed multiple myeloma. Br J Haematol 2009;145:681–708.
40. Podar K, Anderson KC. The pathophysiologic role of VEGF in hematologic malignancies: therapeutic implications. Blood 2005;105:1383–95.
41. Zetser A, Bashenko Y, Edovitsky E, Levy-Adam F, Vlodavsky I, Ilan N. Heparanase induces vascular endothelial growth factor expression: correlation with p38 phosphorylation levels and Src activation. Cancer Res 2006;66:1455–63.
42. Andersen NF, Standal T, Nielsen JL, Heickendorff L, Borset M, Srensen FB, et al. Syndecan-1 and angiogenic cytokines in multiple

myeloma: correlation with bone marrow angiogenesis and survival. Br J Haematol 2005;128:210–7.
43. Seidel C, Borset M, Turesson I, Abildgaard N, Sundan A, Waage A. Elevated serum concentrations of hepatocyte growth factor in patients with multiple myeloma. The Nordic Myeloma Study Group. Blood 1998;91:806–12.
44. Derksen PWB, Keehnen RMJ, Evers LM, van Oers MHJ, Spaargaren M, Pals ST. The cell surface proteoglycan syndecan-1 mediates hepatocyte growth factor binding and promotes met signaling in multiple myeloma. Blood 2002;99:1405–10.
45. Belotti D, Paganoni P, Manenti L, Garofalo A, Marchini S, Taraboletti G, et al. Matrix metalloproteinases (MMP9 and MMP2) induce the release of vascular endothelial growth factor (VEGF) by ovarian carcinoma cells: implications for ascites formation. Cancer Res 2003;63:5224–9.
46. Yang Y, Yaccoby S, Liu W, Langford JK, Pumphrey CY, Theus A, et al. Soluble syndecan-1 promotes growth of myeloma tumors in vivo. Blood 2002;100:610–7.
47. Kato M, Wang H, Kainulainen V, Fitzgerald ML, Ledbetter S, Ornitz DM, et al. Physiological degradation converts the soluble syndecan-1 ectodomain from an inhibitor to a potent activator of FGF-2. Nat Med 1998;4:691–7.
48. Seidel C, Brset M, Hjertner O, Cao D, Abildgaard N, Hjorth-Hansen H, et al. High levels of soluble syndecan-1 in myeloma-derived bone marrow: modulation of hepatocyte growth factor activity. Blood 2000;96:3139–46.
49. Beauvais DM, Ell BJ, McWhorter AR, Rapraeger AC. Syndecan-1 regulates alphavbeta3 and alphavbeta5 integrin activation during angiogenesis and is blocked by synstatin, a novel peptide inhibitor. J Exp Med 2009;206:691–705.
50. Khotskaya YB, Dai Y, Ritchie JP, MacLeod V, Yang Y, Zinn K, et al. Syndecan-1 is required for robust growth, vascularization, and metastasis of myeloma tumors in vivo. J Biol Chem 2009;284:26085–95.
51. Reijmers RM, Groen RW, Rozemuller H, Kuil A, de Haan-Kramer A, Csikós T, et al. Targeting EXT1 reveals a crucial role for heparan sulfate in the growth of multiple myeloma. Blood 2010;115:601–4.